Earth's Future

RESEARCH ARTICLE
10.1029/2018EF001089

A Coherent Statistical Model for Coastal Flood Frequency Analysis Under Nonstationary Sea Level Conditions

Mahshid Ghanbari[1], Mazdak Arabi[1], Jayantha Obeysekera[2], and William Sweet[3]

[1]Department of Civil and Environmental Engineering, Colorado State University, Fort Collins, CO, USA, [2]Sea Level Solutions Center (SLSC), Florida International University, Miami, FL, USA, [3]Center for Operational Oceanographic Products and Services, National Oceanic and Atmospheric Administration, Silver Spring, MD, USA

Key Points:
- A mixture probability model is developed to simultaneously assess the frequency of acute and chronic coastal flooding under higher mean sea levels
- The frequency amplification of minor and major flooding varies by coastal regions
- Pacific coast regions should expect the highest major flood frequency amplification

Supporting Information:
- Supporting Information S1

Correspondence to:
M. Ghanbari,
mahshid.ghanbari@colostate.edu

Citation:
Ghanbari, M., Arabi, M., Obeysekera, J., & Sweet, W. (2019). A coherent statistical model for coastal flood frequency analysis under nonstationary sea level conditions. *Earth's Future*, *7*, 162–177. https://doi.org/10.1029/2018EF001089

Received 1 NOV 2018
Accepted 30 JAN 2019
Accepted article online 4 FEB 2019
Published online 26 FEB 2019

Abstract Flood exposure is increasing in coastal communities due to rising sea levels. Understanding the effects of sea level rise (SLR) on frequency and consequences of coastal flooding and subsequent social and economic impacts is of utmost importance for policymakers to implement effective adaptation strategies. Effective strategies may consider impacts from cumulative losses from minor flooding as well as acute losses from major events. In the present study, a statistically coherent Mixture Normal-Generalized Pareto Distribution model was developed, which reconciles the probabilistic characteristics of the upper tail as well as the bulk of the sea level data. The nonstationary sea level condition was incorporated in the mixture model using Quantile Regression method to characterize variable Generalized Pareto Distribution thresholds as a function of SLR. The performance validity of the mixture model was corroborated for 68 tidal stations along the Contiguous United States (CONUS) coast with long-term observed data. The method was subsequently employed to assess existing and future coastal minor and major flood frequencies. The results indicate that the frequency of minor and major flooding will increase along all CONUS coastal regions in response to SLR. By the end of the century, under the "Intermediate" SLR scenario, major flooding is anticipated to occur with return period less than a year throughout the coastal CONUS. However, these changes vary geographically and temporally. The mixture model was reconciled with the property exposure curve to characterize how SLR might influence Average Annual Exposure to coastal flooding in 20 major CONUS coastal cities.

1. Introduction

The global mean sea level (MSL) has been increasing over the past decades (IPCC, 2014). The rate of sea level rise (SLR) is anticipated to continue to accelerate globally and regionally over the 21st century (Howat et al., 2007; Rahmstorf, 2007; Sweet et al., 2017). Consequently, many coastal regions will be increasingly exposed to frequent coastal flood inundation (Walsh et al., 2014). Coastal communities are particularly vulnerable to SLR due to risks from acute storm surge as well as chronic tidal flooding events. The implications of SLR may include increases in severity and frequency of coastal flooding (Rahmstorf & Coumou, 2011; Ray & Foster, 2016), posing enormous socioeconomic implications in coastal cities (Aerts et al., 2014; Hallegatte et al., 2013; Hinkel et al., 2013). Thus, a coherent assessment of the chronic and acute impacts of SLR on coastal flooding is vital for security of coastal communities.

SLR reduces the freeboard between high water levels (either from tide or storm surge) and local flood thresholds, causing to increase the frequency of both minor (Dahl et al., 2017; Moftakhari et al., 2015; Sweet et al., 2014; Vandenberg-Rodes et al., 2016) and major (Ezer & Atkinson, 2014; Kemp & Horton, 2013; Vousdoukas et al., 2017) coastal flood events. Thus, quantification of risks from coastal flooding under nonstationary sea level conditions must reconcile the effects of both minor and major floods. Development of effective adaptation and mitigation strategies must take into account the cumulative losses from frequent smaller high-water levels (i.e., minor flooding) as well as acute losses from less frequent extreme high-water levels (i.e., major flooding). A challenge, however, is the inadequacy of widely used probability models in simultaneous characterization of both minor and major flooding under higher MSLs.

Literature is replete with probabilistic methods to characterize the likelihood of major flooding under nonstationary condition. Chief among these approaches is the nonstationary Generalized Extreme Value (GEV) distribution and Generalized Pareto Distribution (GPD). Nonstationarity of sea level conditions is typically taken into account by time-dependent distribution parameters for GEV (Boettle et al., 2013; Menéndez &

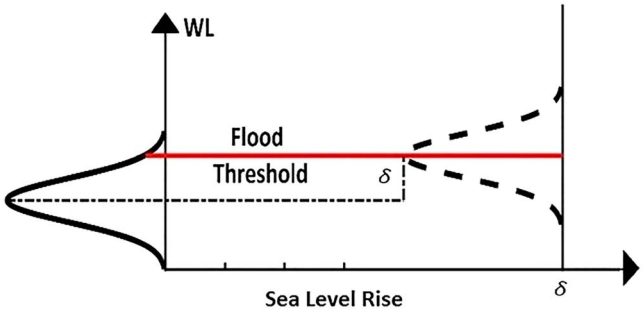

Figure 1. Schematic of changes in water level probability distribution with a δ increase in mean sea level.

Woodworth, 2010; Obeysekera et al., 2013; Salas & Obeysekera, 2014) or GP (Kyselý et al., 2010; Méndez et al., 2006) distributions. The increasing frequency of minor flooding due to SLR has motivated several recent studies (Dahl et al., 2017; Moftakhari, AghaKouchak, et al., 2017; Sweet et al., 2014, 2018). However, most of these previous studies model minor and major flood events separately.

Two important considerations must be addressed to fully characterize acute and chronic flooding risks in a statistically rigorous manner under nonstationary condition. First, using time as a covariate in nonstationary probability models poses planning and management challenges since future SLR projections are fraught with uncertainty. Considerable scientific discourse still remains how to statistically detect SLR acceleration over time (Haigh et al., 2014; Nicholls & Cazenave, 2010). Moreover, local factors such as land subsidence, changes in ocean circulation, and groundwater pumping may also considerably alter the rate of SLR in a region (Konikow, 2011; Ezer et al., 2013). In addition, selecting a meaningful SLR scenario is not a straightforward task, and several factors should be weighed by policymakers and coastal planners to select an appropriate SLR such as the decision type, planning horizon, and overall risk tolerance (Hall et al., 2016; Sweet et al., 2017). Thus, since extreme sea level data are correlated with MSL (Tebaldi et al., 2012), nonstationarity may be addressed in terms of changing in MSL instead of time.

Further, Extreme Value (EV) distributions are commonly used to characterize the tail of water level data (Menéndez et al., 2008; Niroomandi et al., 2018; Noto & La Loggia, 2009; Roth et al., 2012; Xu & Huang, 2008). However, with higher sea levels, current local flood thresholds are likely to be exceeded more frequently during average high tides. Flood events that are currently characterized as infrequent and are mostly modeled by the upper tail of the sea level distribution will become more frequent with SLR and will not be rare events anymore. Thus, in the absence of coastal adaptation measures, water level exceedances above the current flood threshold cannot be characterized using models that characterize only the upper tail of the water level distribution. This limitation impedes full characterization of risks from coastal flooding under nonstationary sea level conditions. Thus, requisite to a full characterization of flood risks is an approach that reconciles the probabilistic characteristics of the upper tail as well as the bulk of the sea level distribution (Stephens et al., 2018).

This study develops a statistically coherent nonstationary mixture probability model for sea water levels to facilitate coastal flood frequency analysis. Specifically, the objectives of the study are to (1) develop and corroborate a nonstationary Mixture Normal-GPD probability model with changes in MSL as the covariate; (2) evaluate current and future coastal flood return periods for regions along the coastal Contiguous United States (CONUS); (3) investigate changes in the frequency of minor and major coastal flooding for the stations along the coastal CONUS; and (4) quantify current and future exposure to coastal flooding in 20 coastal cities in the CONUS. The new mixture probability model enhances the capacity to simultaneously investigate minor and major coastal flooding frequency under future SLR scenarios. The study also investigates the time to anticipated SLR levels on a decadal basis.

2. Materials and Methods

Current local flood thresholds will be exceeded more frequently under higher MSL, which can ultimately result in inadequacy of the extreme value distributions (Figure 1). We developed a nonstationary Mixture Normal-GPD model to enable full characterization of coastal flood frequency with SLR as the covariate. In the mixture model, the Normal distribution describes the bulk of daily maximum sea levels, while GPD characterizes the upper tail of the data. Nonstationarity was incorporated by expressing the location parameters of both Normal distribution and GP distribution as a function of SLR. The model was corroborated for 68 tidal monitoring locations along the coastal CONUS with long-term observed water level data. We used the mixture probability model to assess the effects of SLR on future coastal flood frequency along the coastal CONUS. Subsequently, we reconciled the model with exposure curve for coastal assets (i.e., property value of buildings) in 20 coastal cities to quantify the Average Annual Exposure (*AAE*) of assets to minor and

extreme coastal flooding over a range of SLR levels. Finally, recent regional SLR projections were used to investigate how far in the future changes in frequency of coastal flooding may be realized.

2.1. Tidal Stations, Study Cities, and Projected SLR Scenarios

We used three sets of data in this study to estimate current and future coastal flood frequency and conduct property exposure analysis along the coastal CONUS. First, we used hourly observed sea level data from 68 stations with at least 30 years of data to develop and corroborate the mixture probability model. These stations are located along CONUS coasts, including northeast Atlantic, southeast Atlantic, Gulf, and Pacific coasts. The data represent Still Water Elevation, which encompass both tide and storm components. All the hourly observed water level data are relative to the latest National Tidal Datum Epoch, which references the 1983–2001 period with mean higher high water (MHHW) as the tidal datum except the data from two stations along the Gulf coast (Grand Isle and Rockport tidal stations), which are on the modified epoch. We modified the hourly time series that correspond to these two stations to take the sea level data back onto the 1983–2001 epoch (Sweet et al., 2018).

Second, we selected 20 populated cities along the coastal CONUS, which cover a variety of geographic coastal regions (five cities in each coastal region). All of the cities are highly exposed areas to coastal flooding in terms of infrastructure and other properties. For each city, we used cumulative property exposure values that correspond to water level above MHHW from risk finder tool (https://riskfinder.climatecentral.org) provided by Climate Central (2016). We obtained the property exposure values for 10 different water level values (i.e., 1 to 10 ft above MHHW). Exposure values between these data points were modeled by a linear function.

Third, we used two regional SLR projections to perform a decadal assessment of expected time to certain changes in MSLs by 2100. We selected the "Intermediate Low" scenario, which corresponds to 0.5-m global SLR with 73% chance of being exceeded under Representative Concentration Pathway (RCP) 4.5 climate change scenario. We simulated more accelerated SLR conditions using the "Intermediate" scenario with 1-m global SLR and 17% chance of being exceeded under RCP 8.5 climate change scenario (Kopp et al., 2014; Sweet et al., 2017). Antarctic ice sheet instability could transition to more extreme scenarios (i.e., Intermediate-High, High, and Extreme) later in the century. However, those outcomes are less likely to occur. Thus, the results of the present study may be deemed as plausible but conservative estimates compared to other extreme SLR scenarios.

2.2. Minor, Moderate, and Major Coastal Flooding Classification

To secure public safety and take steps to increase coastal cities preparedness level, three "official" coastal flood thresholds have been established by National Oceanic and Atmospheric Association (NOAA). Minor flooding (i.e., exceedances over minor flood threshold) refers to events that can cause minimal damage with public threat and inconvenience. Moderate coastal flooding (i.e., exceedances over moderate flood threshold) has relatively considerable damages to private and commercial property. Major flooding (i.e., exceedances over major flood threshold) is destructive and can cause extensive losses to life and property. These thresholds are defined observationally during flooding events and are available for less than half of NOAA tide gauges in the CONUS (NOAA, 2014).

A recent study done by Sweet et al. (2018) found a common pattern between all official NOAA coastal flood thresholds based on the local tide range such that in the most cases minor, moderate, and major coastal flooding begin about 0.5, 0.8, and 1.2 m above the local diurnal tide range. Consequently, they estimate a "derived" set of flood threshold based on the statistical relationship (regression-based) for nearly all stations along the coastal CONUS. In this study, we used these set of derived coastal flood thresholds for each station as an approximation of minor, moderate, and major flooding thresholds, which are spatially consistent and can provide national coverage (Sweet et al., 2018).

2.3. Mixture Normal-GPD Probability Model

We developed a nonstationary mixture model that simultaneously characterize the bulk and upper tail of the sea water level distribution. The six parameter models represent extreme values by a GPD and bulk data by a Normal distribution. We estimated the parameters of the mixture model for the 68 tidal monitoring stations along the coastal CONUS.

2.3.1. Extreme Value Analysis

Extreme Value Analysis is commonly used to characterize extreme events with two primary methods for selecting extremes: peak over threshold and block maxima method (e.g., annual maxima). The block maxima approach and corresponding probability models such as the GEV distribution can only consider one event per block (e.g., year). However, coastal flooding, particularly minor flooding events, may occur with multiple occurrences in a year (Moftakhari et al., 2015; Ray & Foster, 2016). Hence, we used the peak over threshold method in the current study to consider multiple events per year. In this approach, a threshold is determined to describe statistical properties of events that exceed the threshold over a given period of time. The cumulative distribution (G) of the independent exceedances above the threshold follow the GPD which is given by (Coles, 2001)

$$G_{u,\alpha,\xi}(x) = \Pr(X \le x | X > u) = \begin{cases} 1-\left(1+\xi\frac{x-u}{\alpha}\right)^{-\frac{1}{\xi}} & if\ \xi \neq 0 \\ 1-\exp\left(-\frac{x-u}{\alpha}\right) & if\ \xi = 0 \end{cases}, \quad (1)$$

where u, α, and ξ denote the location, scale, and shape of the GPD distribution.

2.3.2. Mixture Normal-GPD Distribution

The bulk of daily maximum sea level closely follows a Normal distribution (Sweet & Park, 2014). Thus, using the idea of extreme value mixture model (Behrens et al., 2004), the GPD model for the data above the threshold is mixed with a Normal distribution for the data below the threshold to derive a single-spliced distribution that coherently characterizes probability density of the entire range of sea level data. The cumulative distribution function of the mixture model is defined as (MacDonald et al., 2011)

$$F(x|\mu,\sigma,u,\alpha,\xi,\varphi) = \begin{cases} (1-\varphi)\ \frac{N\ (x|\ \mu,\sigma)}{N\ (u|\ \mu,\sigma)} & if\ x < u \\ (1-\varphi) + \varphi G(x|u,\alpha,\xi) & if\ x \ge u \end{cases}, \quad (2)$$

where $N(x|\,\mu,\sigma)$ and $G(x|\,u,\alpha,\xi)$ are the Normal and conditional GPD cumulative distribution functions, respectively. Variables μ and σ represent mean and standard deviation of the Normal distribution, and φ denotes the probability of independent exceedances over threshold. Variable φ is the ratio of number of clusters above threshold to the total number of observations (Coles, 2001). We used the Maximum Likelihood Estimation (MLE) in MATLAB (MathWorks®) to estimate parameters of the mixture model for the study locations.

2.4. Characterization of Nonstationary Sea Water Level

The effects of SLR must be considered in both components of the Mixture Normal-GPD model. Hence, in the proposed approach, the location parameter of the Normal distribution (μ) and the location parameter of the GPD (u) are expressed as functions of changes in MSL (δ). Climate change may also beget changes in storminess of events (i.e., the frequency and intensity of storms) that cause coastal flooding (Wolf & Woolf, 2006) leading to changes in other parameters (e.g., scale and shape parameter) of water level distribution (Arns et al., 2017; Devlin et al., 2017; Wahl, 2017). However, the changes in storminess were not included in this study for two reasons: (1) previous studies have observed that SLR has more immediate threat for the increase in exceedances over flood thresholds than possible changes in storm variability (Church et al., 2013; Sweet & Park, 2014; Tebaldi et al., 2012); (2) although increase in storminess could change extreme events accompanied with storm surge, as sea levels rise, most of coastal floodings start at normal high tides, with no additional effect of severe weather such as storm or hurricane. The approach assumes that SLR will shift the current sea level distribution toward higher water level without any deformation of the distribution (Le Cozannet et al., 2015; Mudersbach & Jensen, 2010; Tebaldi et al., 2012). Thus, no additional covariate dependency was assumed for scale parameter of Normal component as well as scale and shape parameters of the GP component.

The location parameter of GPD may be represented by either choosing a constant or a variable threshold. When a constant threshold is used, exceedances of the threshold occur more frequently in future years, which may violate the assumption of extreme value analysis (Coles, 2001). Hence, we computed a variable GPD threshold using Quantile Regression method (Koenker & Hallock, 2001; Kyselý et al., 2010). The

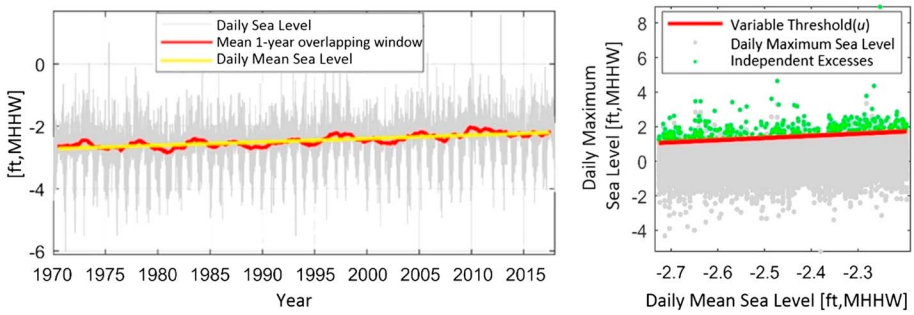

Figure 2. (left) Daily mean sea level calculated using linear function fitted to the daily sea levels, (right) Variable threshold estimated using Quantile regression method and independent excesses over threshold (Battery [NY] tidal station). MHHW = mean higher high water.

analysis determines the relationship between daily MSL (independent variable) and daily maximum sea level (response variable) data. Daily MSLs (DMSL) were computed from the linear model fitted to the daily sea levels (i.e., daily time series of mean of hourly observed water levels; Figure 2, left panel). The linear model (Yellow line) was used instead of daily MSL time series, which was computed from the mean of daily values for 1-year overlapping windows centered at the indicated day (Red line), to remove the noise component in the time series and avoid having sample variability. We assume DMSL correspond to 183rd day of the year 2017 as current DMSL and present all the computed DMSLs as sum of current DMSL and changes in MSL ($DMSL_{\text{current}} + \delta$). Eventually, we calculated the GPD variable threshold as the 97% (Méndez et al., 2006; Sweet et al., 2014) quantile regression assuming linear dependence between daily maximum sea level and DMSL (Figure 2, right panel). The nonstationary characterization of GPD threshold includes two components and is a function of changes in MSL (δ) according to the following equation:

$$u = u(\delta) = \beta_1(\, DMSL_{\text{current}} + \delta) + \beta_0 = \beta_1\delta + (\beta_0 + \beta_1 \times DMSL_{\text{current}}), \tag{3}$$

where u denotes the value of the variable GPD threshold, $DMSL_{\text{current}}$ represents the daily MSL corresponding to the current (i.e., reference) year, β_1 and β_0 denote the slope and intercept coefficients of the quantile regression model, and δ represent change in MSL from the current level. Year 2017 is used as the reference year in the study. The quantile regression coefficients are assumed to remain constant over the range of MSLs.

The estimated slope coefficient (β_1) indicates the rate of change in the GPD threshold, which is used to characterize extremes, with changes in MSL. When β_1 is greater than 1, the changes in extreme values are greater than changes in MSL itself. Conversely, a β_1 value less than 1 points to smaller changes in extremes relative to changes in MSL.

The MLE technique requires independent observations of extremes for robust estimation of GPD parameters. Thus, a minimum time interval between water level extremes (i.e., threshold exceedances) must be identified such that the resulting sequences are statistically independent. In the current study, we employed a minimum of 3-day runs (Méndez et al., 2006; Sweet et al., 2014). The maximum of successive extremes within each cluster was used to estimate GPD parameters (Figure 2, right panel).

Similarly, the nonstationary component for the bulk of the distribution is incorporated by changing the location parameter of the Normal component of the distribution as follows:

$$\mu = \mu(\delta) = \mu_0 + \delta, \tag{4}$$

where μ_0 represents the estimated Normal distribution location parameter computed from historical daily maximum sea level.

2.5. Coastal Flood Frequency and Amplification Factor

The relation between coastal flood level and return period will change under nonstationary conditions (Church et al., 2006; Lin et al., 2012), and subsequently, the frequency of exceedance of a given flood

threshold will increase (Dahl et al., 2017). The annual frequency (expected number of days per year) of exceedances above coastal flooding thresholds (n_e) can be obtained from the mixture probability model as follows:

$$n_e = \frac{1}{T} = \begin{cases} n_y\left(1 - \left[\frac{(1-\varphi)}{1+\mathrm{erf}\left(\frac{u-\mu}{\sigma\sqrt{2}}\right)}\left(1+\mathrm{erf}\left(\frac{x-\mu}{\sigma\sqrt{2}}\right)\right)\right]\right) & x<u \\ \varphi n_y\left(1+\xi\frac{x-u}{\alpha}\right)^{-\frac{1}{\xi}} & x\geq u \end{cases}, \quad (5)$$

where T denotes the return period, ny is the number of observations per year, and *erf* is the error function.

While the frequency of coastal flooding increases with SLR, changes in the frequency of minor and major flooding may not be the same everywhere. Thus, the effect of SLR on changes in frequency of minor and major flooding across coastal regions in the CONUS were assessed using the flood frequency amplification factor (*AF*), which is defined as the ratio of current to future return period of a given water level under a specific SLR (Buchanan et al., 2017):

$$AF = \frac{T_0(x)}{T_\delta(x)}, \quad (6)$$

where $T_0(x)$ is the current return period of water level (x), and $T_\delta(x)$ is the return period of water level (x) under a δ increase in MSL.

2.6. AAE to Coastal Flooding

Flood risk computation involves quantification of flood probability, assets (or other values) at risk, and vulnerability (Kron, 2005; Merz et al., 2010). A widely used risk indicator for flood risk assessment is the Average Annual Losses (Kron, 2005; Purvis et al., 2008). However, in this study, we used the exposure values as an approximation of damages due to many uncertainties in estimating damages across different types of flooding, especially indirect losses in the case of minor flooding. Thus, we estimated *AAE* of property to "minor" and "moderate and major" coastal flooding in 20 major CONUS coastal cities. Here we use the term "extreme" flooding to refer to moderate and major flooding since both flooding categories can cause considerable damage to property (NOAA, 2014). *AAE* to minor and extreme (i.e., moderate and major) flooding is determined by

$$AAE\ \text{Extreme} = \int_0^{1-F(\text{Moderate Flood Threshold})} n_y{*}E\left(F^{-1}(1-p)\right)\mathrm{d}p, \quad (7a)$$

$$AAE\ \text{Minor} = \int_{1-F(\text{Moderate Flood Threshold})}^{1-F(\text{Minor Flood Threshold})} n_y{*}E\left(F^{-1}(1-p)\right)\mathrm{d}p \quad (7b)$$

where E denotes the exposure function, and p represents the sea level exceedance probability. The *AAE* to minor and major flooding was computed for 20 cities along the coastal regions in CONUS for various SLR levels.

3. Results

The study reveals that minor and major flood frequencies generally increase as sea level rises; however, these changes vary geographically along the coastal CONUS. Major flood frequency amplification is primarily governed by the value of shape parameter. In regions with negative or close to zero shape parameter (i.e., Pacific and Southeast Atlantic coasts), major flood frequency amplification is more sensitive to SLR and is higher than minor flood frequency amplification. On the contrary, locations with large positive shape parameter (i.e., Gulf and northeast Atlantic coasts) are anticipated to be exposed to higher frequency amplification in minor flooding. Considering regional SLR projections, events currently classified as major flooding are anticipated to occur with return period less than a year in all stations by the end of the century under Intermediate SLR scenario.

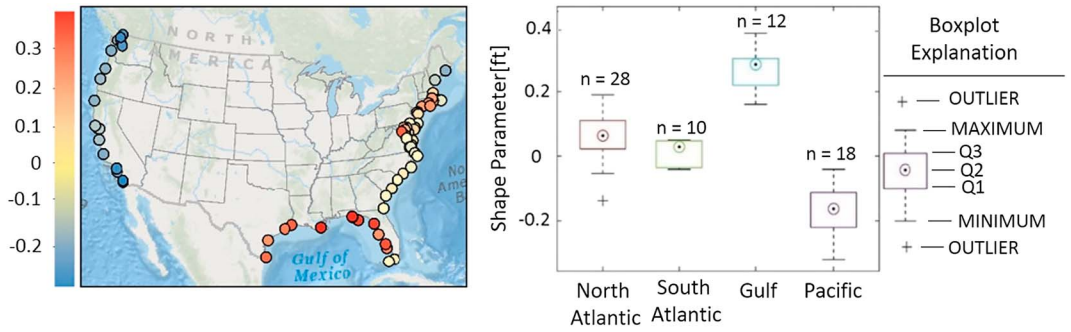

Figure 3. (left) Geographical distribution of Generalized Pareto Distribution shape parameter. (Right) Boxplot of Generalized Pareto Distribution shape parameter (Q1, Q2, and Q3 indicate lower quartile, median, and higher quartile, respectively, and *n* denotes the number of stations).

3.1. Parameters of the Mixture Model by Region

The mixture model parameter values for all 68 tidal stations were estimated using the MLE method and are summarized in supporting information Table S1. The GPD shape parameter governs the qualitative behavior of GPD distribution (Coles, 2001). When the shape parameter is positive ($\xi > 0$), the distribution is heavy-tailed and has no upper bound. Conversely, when $\xi < 0$, the distribution is thin-tailed and has upper limit equal to $x_{\max} = u - \frac{\alpha}{\xi}$.

The estimated shape parameters for the stations along the coastal CONUS reveal important regional patterns (Figure 3). Figure 3 (right panel) presents the boxplot of GPD shape parameters in each region. From this boxplot, it can directly be observed that locations along Gulf and Pacific coasts have the highest and lowest GPD shape parameter, respectively, and the median is almost equal to zero for stations along the southeast Atlantic coasts. The shape parameters for stations along the Pacific coast region are negative ranging between −0.02 and −0.1 or highly negative with values less than −0.1. These stations historically do not experience tropical cyclone or hurricanes and have a very narrow continental shelf that limits storm surge potential. On the other hand, stations along the Gulf and northeast Atlantic regions are exposed to tropical cyclones and strong winter storms, respectively. The shape parameter for these stations is highly positive with values more than 0.1 or positive ranging between 0.02 and 0.1. Stations along southeast Atlantic region experience differing degrees of exposure to tropical storms with the shape parameter approximately zero with values in the range of −0.02 to 0.02. It is clear that different experience among stations in terms of historical exposure to extreme flooding can be reflected by GPD shape parameter (Buchanan et al., 2017).

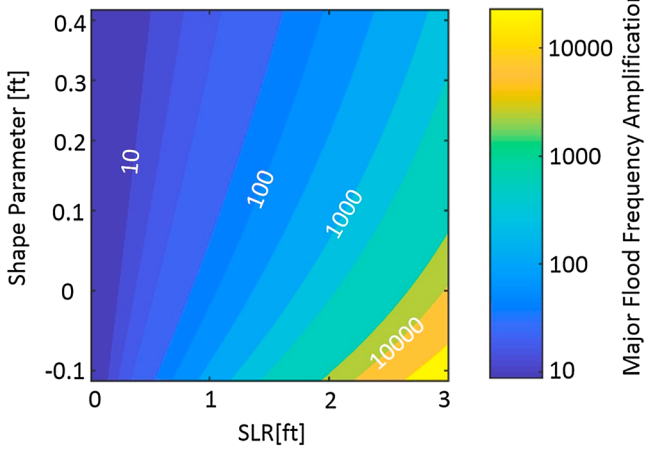

Figure 4. Sensitivity of major flood frequency amplification with SLR and the distribution shape parameter. SLR = sea level rise.

Local characteristic of tidal stations could also affect the value of GPD shape parameter. For example, Key West and Vaca Key (Florida Keys) stations, which are located close to the margins of continental shelf zones, similar to the situation along the Southwestern Pacific coast, tend to be exposed to lower surge compared to stations that are located behind the wide shelves. Moreover, stations close to estuaries may be also exposed to relatively high storm surge or large riverine inputs (e.g., Washington DC station; Tebaldi et al., 2012).

The sensitivity of major flood frequency amplification to the shape parameter over a range of SLR levels is illustrated in Figure 4. Other parameters of the distribution and Quantile Regression coefficients were kept constant at $u_0 = 1.8$; $\alpha = 0.4$; $\mu_0 = 0$; $\sigma = 0.8$; $\varphi = 0.02$; $\beta_1 = 1$; $\beta_0 = 7$. Generally, frequency amplification of major flooding is inversely related to the value of shape parameter. As shape parameter increases, major flooding frequency amplification tends to be smaller for changes in MSL. This response is governed by the effects of shape parameter on the tail of sea level distribution and the frequency of extreme flood levels. Distributions with $\xi > 0$ have relatively high frequency of extreme flood

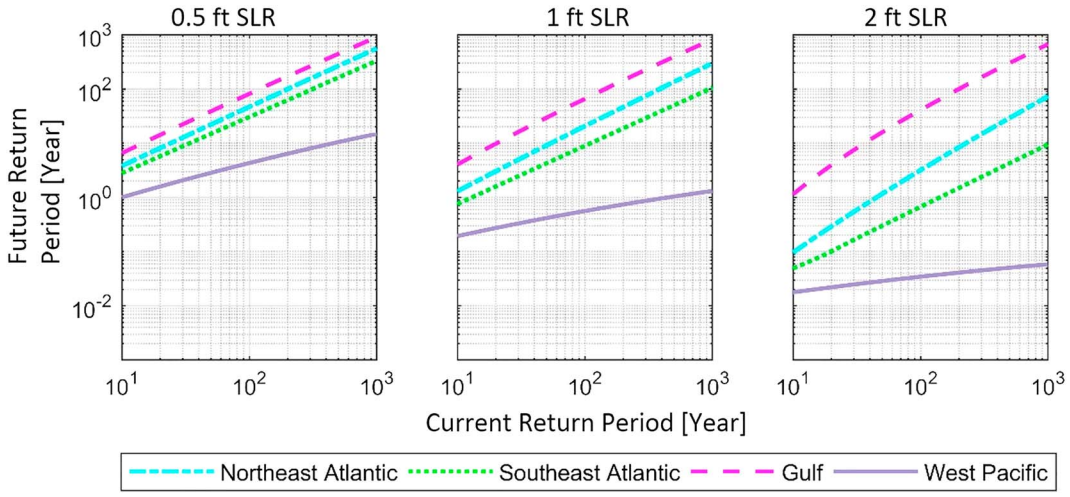

Figure 5. Current versus future coastal flood return period (Median value for each region). SLR = sea level rise.

levels, while distributions with $\xi < 0$ have an upper bound of extreme flood levels. When shape factor is highly negative, for example, for locations where currently major flooding does not occur or is highly unlikely, very large frequency amplifications may be computed.

Conversely, minor flooding frequency amplification is not sensitive to the value of shape parameter. The minor flood threshold typically is not located at the tail of the GPD and is not governed by shape parameter.

3.2. Current and Future Coastal Flooding Return Period

Changes in the return period of future coastal flooding were assessed under different SLR levels in the study locations. The median of these changes by coastal regions is summarized in Figure 5. Figures S2e to S69e provide the results of the analysis for each station. Generally, future return periods will become shorter as the sea level rises. A significant change is determined for study sites in the Pacific region. For example, 500-year flood will become a 10-year, yearly, and monthly flood under 0.5-, 1-, and 2-ft SLR, respectively. However, these changes in flood return period do not necessarily indicate higher exposure and risks in the future since return period alone does not provide sufficient information for risk management policies (Tebaldi et al., 2012). For example, the flood levels for the current 100-year event is about 3 ft for regions along the Pacific coast, posing little flood risks.

To make this point clearer, Figure 6 depicts the estimated future return period for prevailing 100-year coastal flooding events under 0.5-ft (left panel) and 2-ft (right panel) SLR levels. Locations along the Gulf region will experience the highest 100-year depth. On the contrary, the smallest 100-year flood depths are estimated for locations along the Pacific coast, which historically have not been exposed to hurricane and tropical cyclone. A relation is evident between the future return period and current 100-year return level (Tebaldi et al., 2012),

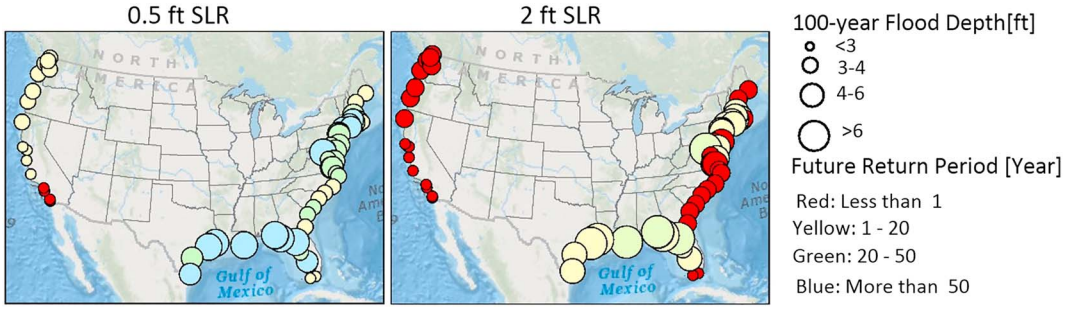

Figure 6. Future 100-year flood return period classified by current 100-year flood depth. The size and color represent the "Future return period" and the "depth" of current 100-year flood, respectively. SLR = sea level rise.

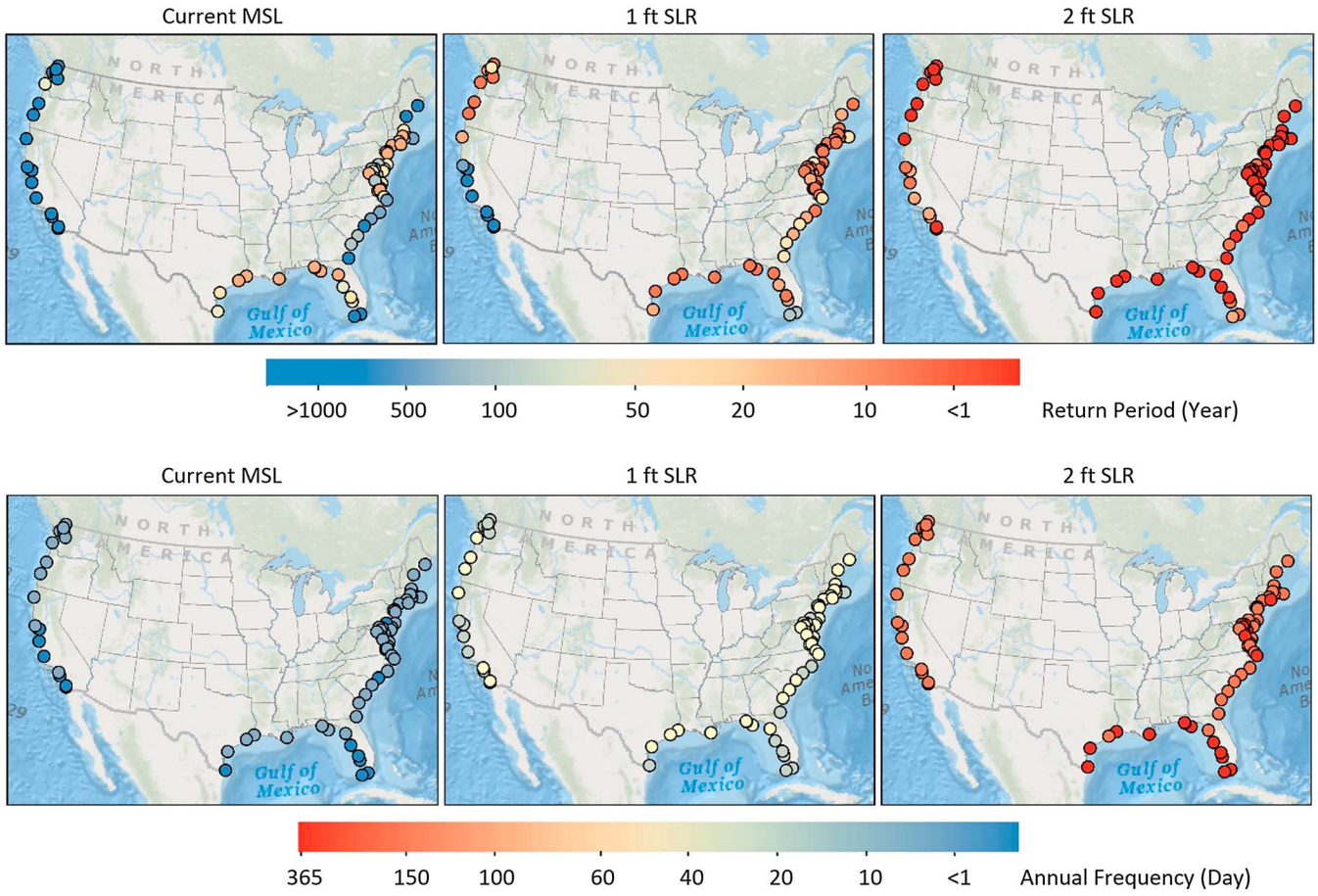

Figure 7. (top panels) Return period of major coastal flooding; (bottom panels) expected annual frequency of minor coastal flooding. MSL = mean sea level; SLR = sea level rise.

which express that changes in return period alone does not provide sufficient information for risk management policies.

3.3. Current and Future Frequency of Minor and Major Coastal Flooding

For more practical use of future return period, we calculated the frequency of minor and major flooding (i.e., exceedances over derived minor and major flood thresholds, respectively) for each station under current and future MSL values. Generally, as sea levels rise, the likelihood of flooding increases should the local flooding thresholds remain constant (Dahl et al., 2017; Kruel, 2016). Figure 7 (top panels) shows estimated future return period for major flooding events, under the current MSL, 1-ft, and 2-ft SLR. Under the current condition, major flooding events occur along the Gulf and northeast Atlantic coasts with a return period less than 100 years. With 1-ft SLR, the large majority of locations (except locations along the southwest Pacific with no exceedances above major flood threshold) tend to be exposed to major flooding with a return period of 1–20 years. Under 2-ft SLR, should no interventions be implemented, major flooding will become commonplace with multiple annual occurrences in most of the CONUS coastal regions.

Annual Frequency (i.e., expected annual number of exceedances) of minor flooding is presented in Figure 7 (bottom panels). Annual frequency of minor flooding was computed instead of return period since multiple minor flooding events may occur within in a year (i.e., return period less than 1 year). Results show that minor flooding currently occurs with the expected number of 1 to 20 days/year in most stations along the Atlantic, Gulf, and Northwest Pacific coasts. Under the current MSL, the least frequency of exceedances is realized with expected annual exceedances of less than 1 day for stations along the southwest Pacific coast

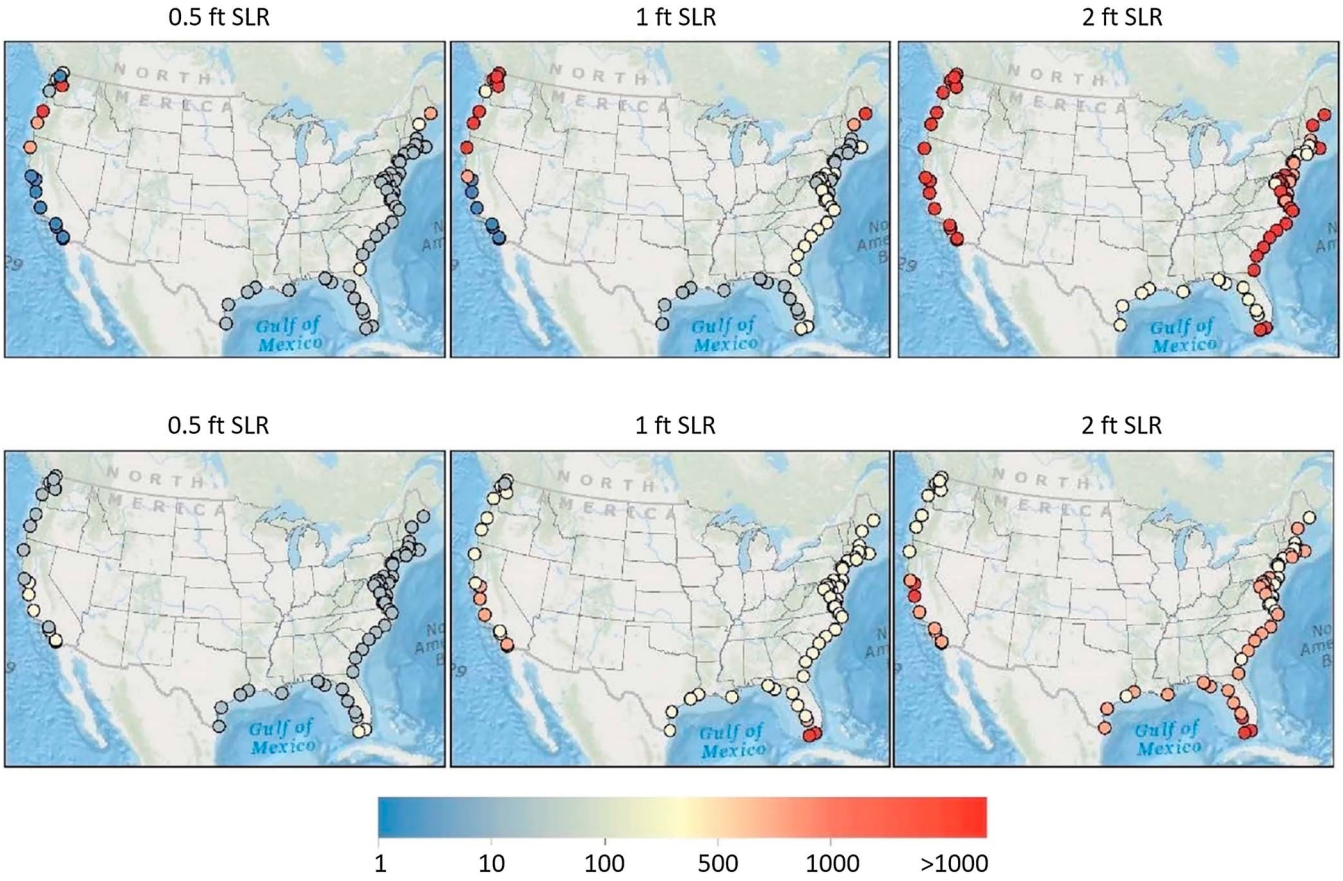

Figure 8. (top panels) Major flood frequency amplification; (bottom panels) minor flood frequency amplification. SLR = sea level rise.

as well as the southwestern coast of Florida. However, 1-ft SLR will culminate in increased frequency of minor flooding to 20–50 days/year in a majority of the study locations. With no adaptations or interventions, 2-ft SLR will result in more than 150 days of minor flooding per year in all the locations.

3.4. Frequency Amplification of Minor and Major Coastal Flooding

Although the frequencies of minor and major flooding are forecasted to increase as a result of SLR, changes in their frequencies are not the same across regions. Thus, frequency amplification of minor and major coastal flooding was calculated for all sites to assess the effect of SLR on changes in the frequency of minor and major flooding separately across different coastal regions (Figure 8).

The frequency amplification of major flooding in the locations along the northwest Pacific will increase substantially with 1-ft SLR. Although the region is not historically exposed to major flooding, the major flood threshold is anticipated to be exceeded by return period of less than 10 years under 1-ft increase in the MSL. With 2-ft SLR, major flood frequency amplification in southwest Pacific will also increase with more than three orders of magnitude. Thus, SLR 2 ft above the current MSL will beget striking amplification of major flooding frequency in all locations along the Pacific and southeast Atlantic. With 0.5-ft SLR, minor flood will become more frequent by up to tenfold in all stations, except those located along southwest Pacific coast and Florida Keys stations with an estimated two orders of magnitude increase. Under 1-ft SLR, the highest amplification in minor flooding (more than 500 times) was found in Florida Keys stations.

We calculated the ratio of major flood frequency amplification to minor flood frequency amplification to investigate patterns of change in flood frequency with SLR in the study regions. Results indicate varying trends by locations across the coastal CONUS (Figure 9). The frequency amplification of minor flooding is higher than major flooding in most of the study locations up to 1-ft SLR except locations along the northwest Pacific coast. Under 2-ft SLR, the frequency of major flooding will be amplified at higher rates in locations

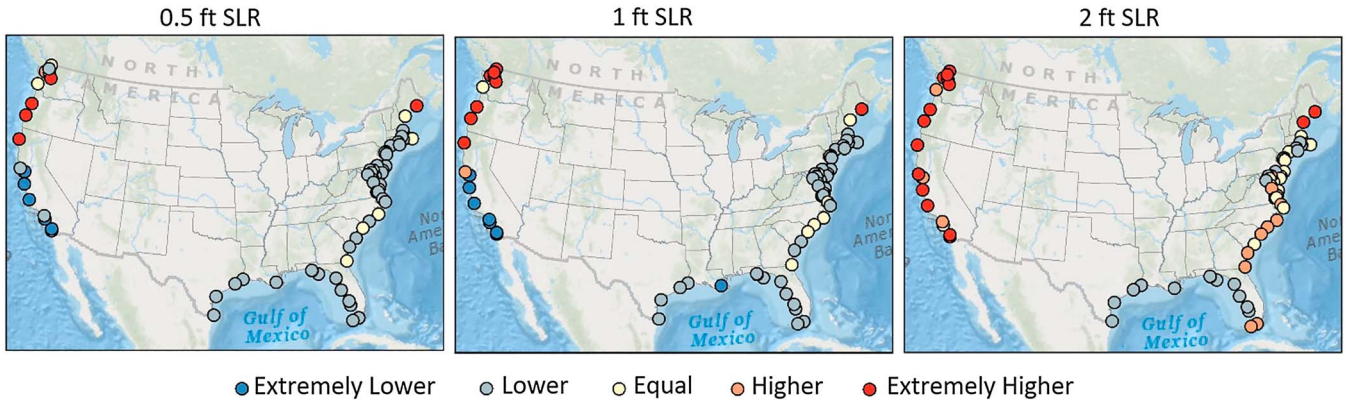

Figure 9. The ratio of frequency amplification of major to minor flooding. SLR = sea level rise.

along the Pacific and southeast Atlantic coasts. Minor flooding frequency, on the other hand, tends to be higher along the Gulf and northeast Atlantic coasts. Thus, as sea level rises locations that historically are not exposed to major flooding are expected to experience higher frequency amplification in major flooding. Coastal areas with considerable historical major flooding will be likely exposed to higher frequency amplification in minor flooding.

3.5. Regional SLR Scenarios for the United States

Observed and projected acceleration of SLR varies regionally across the coastal CONUS. Consequently, the indicated SLR levels in this study are expected to be realized over different time horizons in different coastal

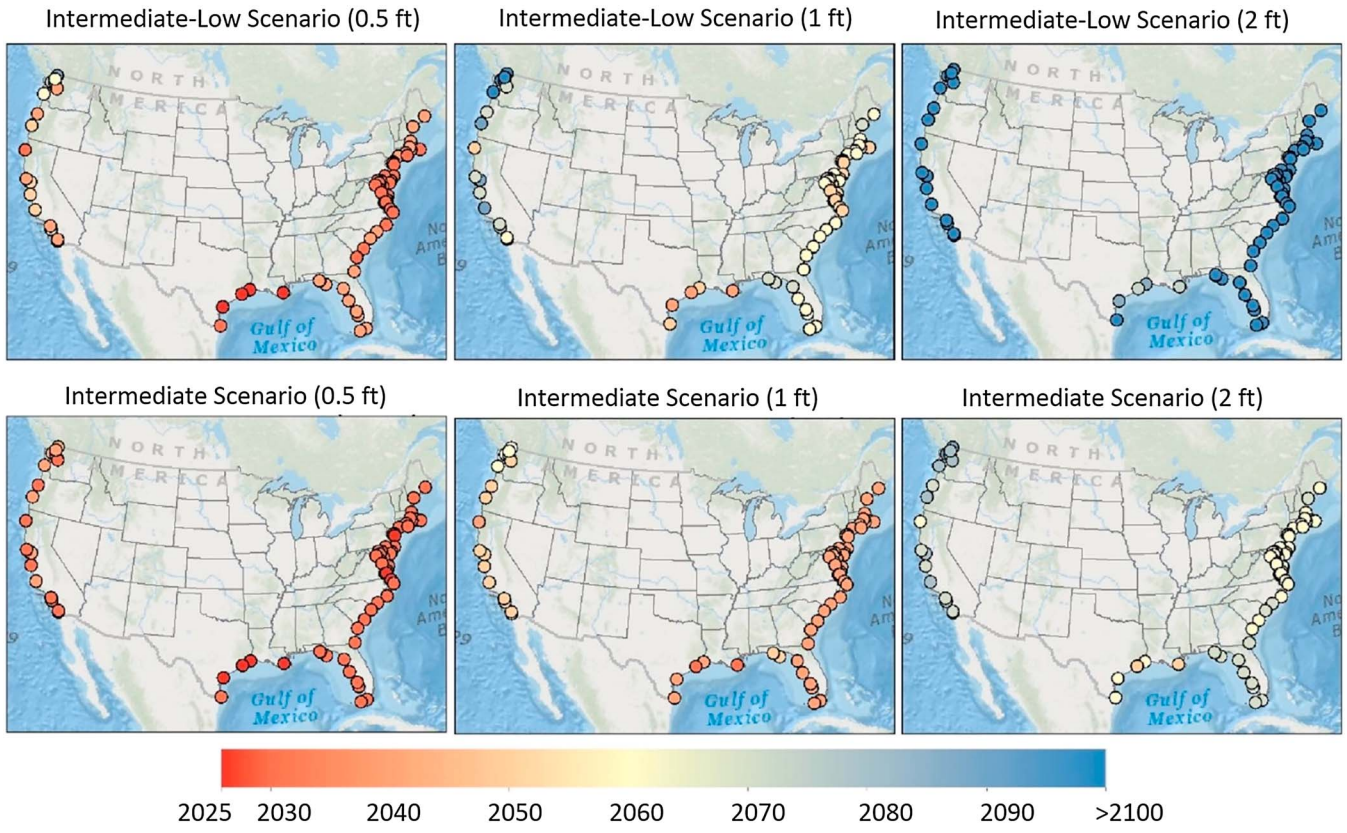

Figure 10. The decade when indicated sea level rise values are anticipated to occur under Intermediate Low and Intermediate sea level rise scenarios (Sweet et al., 2017).

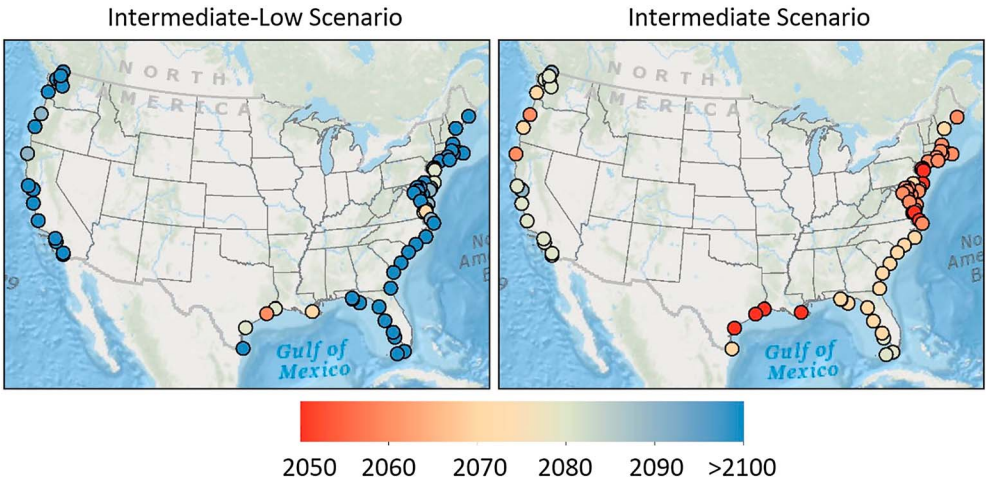

Figure 11. The decade when events currently characterized as major flooding are anticipated to occur with return period less than a year.

locations. Different SLR projections have been derived based on alternative climate scenarios although considerable debate still remains about the acceleration of SLR (Dangendorf et al., 2017; Haigh et al., 2014). Figure 10 (adapted from Sweet et al., 2017) illustrates the decade when the indicated SLR (0.5, 1, and 2 ft) is anticipated to occur under Intermediate Low and intermediate SLR scenarios.

The expected time to frequent destructive major floods with return period of 1 year under Intermediate Low and Intermediate SLR scenarios is illustrated in Figure 11. Under the Intermediate-Low scenario (left panel), most of the stations (except stations along the west of the Gulf coast) will not experience yearly major flooding by the end of the century. However, under the Intermediate scenario, major flooding will occur one or more times a year by approximately 2050–2060 in stations along the western Gulf and mid-Atlantic coasts, 2070–2080 in stations along southeast Atlantic (Except Florida Keys) and some stations along the northwest Pacific, and 2080–2090 in Florida Keys and stations along the southwest Pacific coasts. In general, under the Intermediate scenario, events that are currently characterized as major flooding are anticipated to occur with return period less than a year in all stations by the end of the century.

3.6. AAE to Coastal Flooding

The *AAE* to minor and extreme flooding (i.e., Moderate and major flooding) for 20 populated coastal cities in the CONUS was computed under current condition and three different SLR levels (Figure 12). The *AAE* to both minor and extreme flooding is the highest in the New York City. Although the *AAE* currently is not a major concern for Miami, with 2-ft SLR, Miami will encompass the second highest value of assets exposed to minor and extreme coastal flooding. This response can be attributed to less extreme water-level variance in the Key West station (Church et al., 2013; Hunter, 2012), which is the closest station to Miami in this study.

The ratio of *AAE* to minor flooding to total *AAE* was calculated to explore regional trends in the contribution of each coastal flood category (Figure 13). Under prevailing MSL, extreme coastal flooding accounts for more than 50% of total *AAE* in the cities along the Gulf and northeast Atlantic (e.g., New Orleans and New York City). Minor flooding, however, contributes to more than 50% of total *AAE* in the study cities along the southeast Atlantic and Pacific (e.g., Jacksonville and Los Angeles). Under smaller amounts (up to 1 ft) of SLR, *AAE* will be primarily from minor flooding in all study cities. However, extreme flooding will dominate the coastal flooding *AAE* in most of the CONUS cities for SLR exceeding 2 ft.

These responses can be explained by the components of the mixture probability model. With no rise in MSL, the tail of the sea level distribution (i.e., GPD) governs the contributions from both minor and extreme flooding. Thus, in locations with a positive GPD, shape parameter contributions from acute *AAE* to extreme events exceed chronic *AAE* to minor flooding (i.e., cities along the Gulf coast). On the other hand, cumulative *AAE* from minor flooding is the dominant component of total *AAE* in the study locations with negative GPD shape parameters (i.e., cities along the Pacific coast) due to the thin-tailed distribution. With relatively

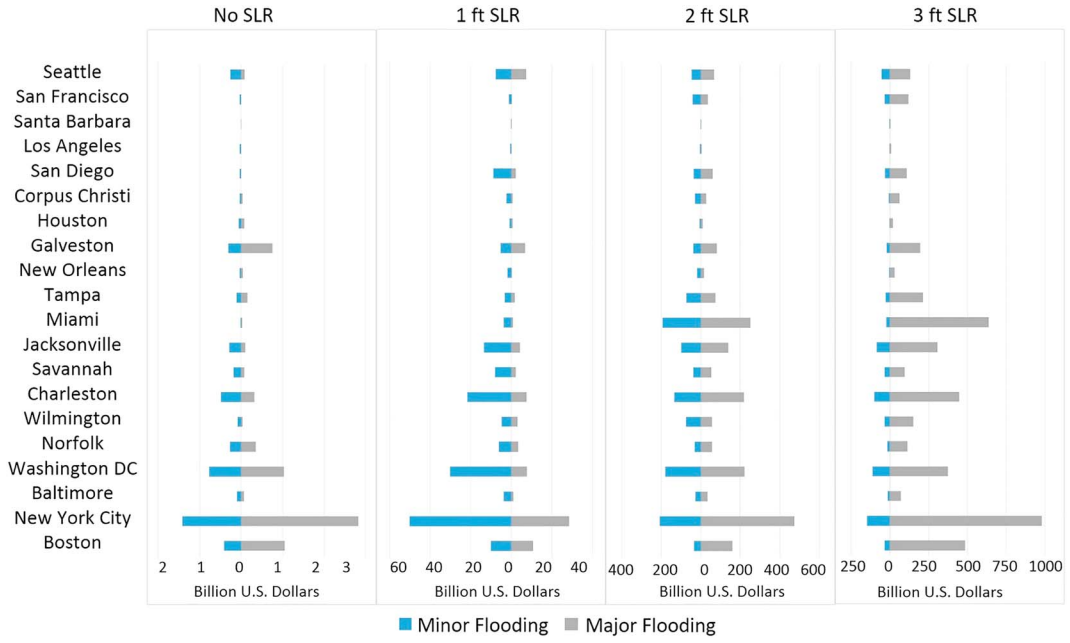

Figure 12. The Average Annual Exposure to minor and extreme flooding in 20 coastal cities along the coastal Contiguous United States. SLR = sea level rise.

small increases (e.g., up to 1 ft) in MSL, a substantial increase in annual exposure to minor flooding is evident. With up to 1-ft SLR, minor flood threshold in all study cities will be smaller than the GPD threshold, and thus, exceedances of the minor flood threshold will be governed by the bulk of the Mixture distribution (i.e., Normal distribution component). Conversely, with SLR above 2 ft, moderate and major flood thresholds will also be shifted to the bulk of the water level distribution, which will lead to a greater portion of *AAE* from extreme flooding events.

Minor flooding can cause considerable indirect damages to assets and economic activities in cities, such as business interruption, road closure, traffic disruptions, economic losses, public inconvenience, and long-term chronic degradation of infrastructure from increasing inundation of saltwater (e.g., Moftakhari et al., 2018; Sweet et al., 2014). We do not consider these impacts in the current study. Moreover, repeated events

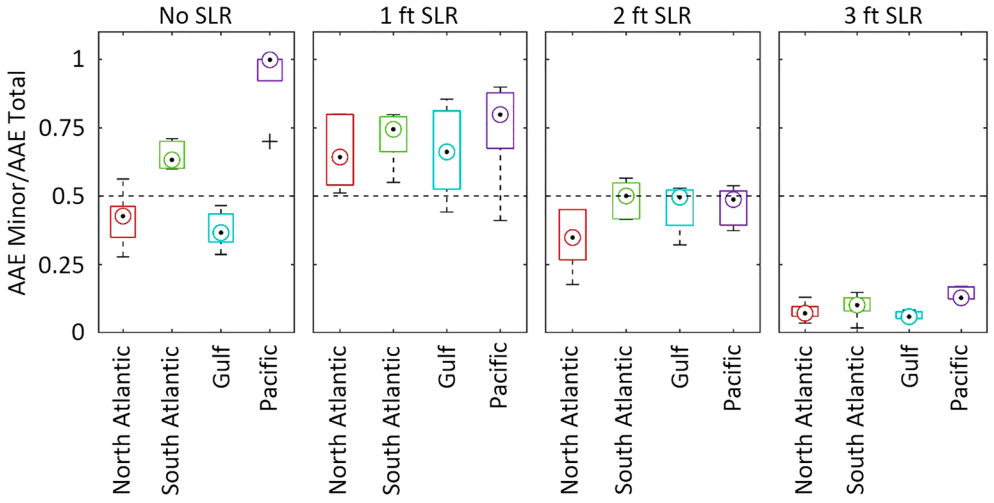

Figure 13. The ratio of *AAE* to minor flooding to total *AAE* for Contiguous United States coastal regions. AAE = Average Annual Exposure; SLR = sea level rise.

of exposure to coastal flooding are assumed to be independent. Thus, the *AAE* used in this study may be viewed as a worst case risk estimate and is likely substantially larger than Average Annual Losses (Hallegatte et al., 2013). Detailed damage and restoration functions may be considered when actual losses are computed using the proposed mixture probability model and risk analysis approach. The nonstationary mixture model improves the capability to assess increasing coastal flood risks due to SLR. However, climate change may alter weather conditions that influence increased risks of pluvial flooding from heavy precipitation (Moftakhari, Salvadori, et al., 2017; Wahl et al., 2015) in addition to storm surge. Further theoretical development is needed to reconcile these compounding effects in the analysis of risks to assets and communities in coastal region.

4. Conclusions

A nonstationary Mixture Normal-GPD probability distribution was developed to model coastal flooding frequency over a range of SLR levels. The model facilitates a coherent assessment of coastal flooding exposure to extreme events as well as minor but more frequent events. The model was parameterized for 68 tidal monitoring stations along the coastal CONUS. The results show a good fit between the model and observed sea level data in all study locations. Regional trends are evident in the estimated values of the mixture model parameters. Particularly, the distribution shape parameter, which governs the qualitative behavior of the models and risks to both chronic and acute flooding hazards, showed strong regional trends.

Model assessments reveal that all regions across coastal CONUS will experience significant increases in frequency of minor and major flooding over a range of future SLR levels. Under higher SLR scenarios (e.g., 2-ft SLR), infrequent major flooding is likely to occur multiple times per year in the majority of stations along Atlantic, Gulf, and northwest Pacific coasts. Similarly, minor flooding with exceedances of more than 150 days/year may also occur in most of the study locations. However, the frequency amplification of minor and major flooding varies by coastal regions. Pacific coast regions should expect the highest major flood frequency amplification followed by regions within the southeast Atlantic coast. These regions, especially within the Pacific coast, are most vulnerable to the amplification of major flooding frequency since under current MSL, the major flood threshold is rarely or never exceeded. On the contrary, the Gulf and northeast Atlantic coastal regions are likely to be exposed to higher frequency amplification in minor flooding.

Flood frequency amplification would exacerbate inundation impacts over time and cause a considerable increase in *AAE* of property to coastal flooding. While the communities have primarily focused on mitigating acute damages from extreme events, under smaller amounts of SLR (i.e., up to 1 ft), the *AAE* to minor flooding will exceed those from extreme events in a majority of CONUS coastal regions. However, *AAE* will be mainly from extreme flooding should SLR exceed 2 ft.

The time to specific SLR scenarios varies regionally and by future climate scenarios. Subsequently, risks from minor and extreme coastal flooding will be influenced by these considerations. Planning and design of effective coastal flooding solutions must incorporate both chronic and acute risks from minor and extreme events from SLR. The mixture probability model and the coastal property exposure analysis presented in this study facilitate full characterization of risk mitigation strategies by representing their effects on flood thresholds in coastal regions. These solutions may include engineering solutions such as higher sea walls and forward pumps or management solutions such as spatial zoning regulations and buildings codes. The analysis indicates that adaptation strategies must account for increasing frequency of unprecedented major flooding in the Pacific and southeast Atlantic regions. In the Gulf and northeast Atlantic coasts, effective infrastructural, policy, and management strategies may also target enhanced long-term service reliability of flood control systems and their resiliency to the amplification of minor flooding.

Acknowledgments
This work was supported by the National Science Foundation (NSF) grant 1444758 as part of the Urban Water Innovation Network (UWIN). The hourly observed water level data for all tide stations across coastal CONUS are available from the National Oceanic and Atmospheric Association (http://tidesandcurrents.noaa.gov/). The local sea level projections are provided by Sweet et al. (2017). The coastal flood thresholds for all the stations are provided by Sweet et al. (2018). The data for property exposure values under different sea levels are obtained from the risk finder tool provided by Climate Central (https://riskfinder.climatecentral.org/).

References

Aerts, J. C. J. H., Botzen, W. J. W., Emanuel, K., Lin, N., & De Moel, H. (2014). Evaluating flood resilience strategies for coastal megacities. *Science*, *344*(6183), 473–475. https://doi.org/10.1126/science.1248222

Arns, A., Dangendorf, S., Jensen, J., Talke, S., & Bender, J. (2017). Sea-level rise induced amplification of coastal protection design heights. *Nature Publishing Group*, *7*(40171), 1–9. https://doi.org/10.1038/srep40171

Behrens, C. N., Lopes, H. F., & Gamerman, D. (2004). Bayesian analysis of extreme events with threshold estimation. *Statistical Modeling*, *4*(3), 227–244. https://doi.org/10.1191/1471082X04st075oa

Boettle, M., Rybski, D., & Kropp, J. P. (2013). How changing sea level extremes and protection measures alter coastal flood damages. *Water Resources Research*, *49*, 1199–1210. https://doi.org/10.1002/wrcr.20108

Buchanan, M. K., Oppenheimer, M., & Kopp, R. E. (2017). Amplification of flood frequencies with local sea level rise and emerging flood regimes. *Environmental Research Letters*, *12*(6). https://doi.org/10.1088/1748-9326/aa6cb3

Church, J. A., Clark, P. U., Cazenave A., Gregory, J. M., Jevrejeva, S., Levermann, A., et al. (2013). Sea level change. Climate Change 2013: The Physical Science Basis. Contribution of Working Group I to the Fifth Assessment Report of the Intergovernmental Panel on Climate Change, 1137–1216. https://doi.org/10.1017/CB09781107415315.026

Church, J. A., Hunter, J. R., McInnes, K. L., & White, N. J. (2006). Sea-level rise around the Australian coastline and the changing frequency of extreme sea-level events. *Australian Meteorological Magazine*, *55*, 253–260. https://doi.org/10.1016/j.gloplachs.2006.04.001

Climate Central. (2016). Surging seas: Risk finder. Retrieved from https://riskfinder.climatecentral.org/

Coles, S. (2001). An introduction to statistical modeling of extreme values.

Dahl, K. A., Fitzpatrick, M. F., & Spanger-Siegfried, E. (2017). Sea level rise drives increased tidal flooding frequency at tide gauges along the U.S. East and Gulf Coasts: Projections for 2030 and 2045. *PLoS One*, *12*(2), e0170949. https://doi.org/10.1371/journal.pone.0170949

Dangendorf, S., Marcos, M., Wöppelmann, G., Conrad, C. P., Frederikse, T., & Riva, R. (2017). Reassessment of 20th century global mean sea level rise. *Proceedings of the National Academy of Sciences of the United States of America*, *114*(23), 1–6. https://doi.org/10.1073/pnas.1616007114

Devlin, A. T., Jay, D. A., Talke, S. A., Zaron, E. D., Pan, J., & Lin, H. (2017). Coupling of sea level and tidal range changes, with implications for future water levels. *Scientific Reports*, *7*(17021). https://doi.org/10.1038/s41598-017-17056-z

Ezer, T., & Atkinson, L. P. (2014). Accelerated flooding along the U.S. East Coast: On the impact of sea-level rise, tides, storms, the Gulf Stream, and the North Atlantic Oscillations. *Earth's Future*, *2*(8), 362–382. https://doi.org/10.1002/2014EF000252

Ezer, T., Atkinson, L. P., Corlett, W. B., & Blanco, J. L. (2013). Gulf Stream's induced sea level rise and variability along the U.S. mid-Atlantic coast. *Journal of Geophysical Research: Oceans*, *118*, 685–697. https://doi.org/10.1002/jgrc.20091

Haigh, I. D., Wahl, T., Rohling, E. J., Price, R. M., Pattiaratchi, C. B., Calafat, F. M., & Dangendorf, S. (2014). Timescales for detecting a significant acceleration in sea level rise. *Nature Communications*, *5*, 1–11. https://doi.org/10.1038/ncomms4635

Hall, J. A., Gille, S., Obeysekera, J., Sweet, W., Knuuti, K., & Marburger, J. (2016). Regional sea level scenarios for coastal risk management: Managing the uncertainty of future sea level change and extreme water levels for Department of Defense Coastal Sites Worldwide., (April) (224 pp.). https://doi.org/10.13140/RG.2.2.31307.39208

Hallegatte, S., Green, C., Nicholls, R. J., & Corfee-Morlot, J. (2013). Future flood losses in major coastal cities. *Nature Climate Change*, *3*. https://doi.org/10.1038/NCLIMATE1979

Hinkel, J., van Vuuren, D. P., Nicholls, R. J., & Klein, R. J. T. (2013). The effects of adaptation and mitigation on coastal flood impacts during the 21st century. An application of the DIVA and IMAGE models. *Climatic Change*, *117*(4), 783–794. https://doi.org/10.1007/s10584-012-0564-8

Howat, I. M., Joughin, I., & Scambos, T. A. (2007). Rapid changes in ice discharge from. *Science*, *315*(5818), 1559–1561. https://doi.org/10.1126/science.1138478

Hunter, J. (2012). A simple technique for estimating an allowance for uncertain sea-level rise. *Climatic Change*, *113*(2), 239–252. https://doi.org/10.1007/s10584-011-0332-1

IPCC (2014). Climate change 2014: Synthesis report. In Core Writing Team, R. K. Pachauri, & L. A. Meyer (Eds.), *Contribution of Working Groups I, II and III to the Fifth Assessment Report of the Intergovernmental Panel on Climate Change* (pp. 1–112). Geneva, Switzerland: IPCC. https://doi.org/10.1017/CBO9781107415324

Kemp, A. C., & Horton, B. P. (2013). Contribution of relative sea-level rise to historical hurricane flooding in New York City. *Journal of Quaternary Science*, *28*(6), 537–541. https://doi.org/10.1002/jqs.2653

Koenker, R., & Hallock, K. F. (2001). Quantile regression. *Journal of Economic Perspectives*, *15*(4), 143–156. https://doi.org/10.1016/B978-0-08-097086-8.42074-X

Konikow, L. F. (2011). Contribution of global groundwater depletion since 1900 to sea-level rise. *Geophysical Research Letters*, *38*, L17401. https://doi.org/10.1029/2011GL048604

Kopp, R. E., Horton, R. M., Little, C. M., Mitrovica, J. X., Oppenheimer, M., Rasmussen, D. J., et al. (2014). Probabilistic 21st and 22nd century sea-level projections at a global network of tide-gauge sites. *Earth's Future*, *2*(8), 383–406. https://doi.org/10.1002/2014EF000239

Kron, W. (2005). Flood risk = hazard values vulnerability. *Water International*, *30*(1), 58–68. https://doi.org/10.1080/02508060508691837

Kruel, S. (2016). The impacts of sea-level rise on tidal flooding in Boston, Massachusetts. *Journal of Coastal Research*, *322*(6), 1302–1309. https://doi.org/10.2112/JCOASTRES-D-15-00100.1

Kyselý, J., Picek, J., & Beranová, R. (2010). Estimating extremes in climate change simulations using the peaks-over-threshold method with a non-stationary threshold. *Global and Planetary Change*, *72*(1–2), 55–68. https://doi.org/10.1016/j.gloplacha.2010.03.006

Le Cozannet, G., Rohmer, J., Cazenave, A., Idier, D., van de Wal, R., de Winter, R., et al. (2015). Evaluating uncertainties of future marine flooding occurrence as sea-level rises. *Environmental Modeling and Software*, *73*, 44–56. https://doi.org/10.1016/j.envsoft.2015.07.021

Lin, N., Emanuel, K., Oppenheimer, M., & Vanmarcke, E. (2012). Physically based assessment of hurricane surge threat under climate change. *Nature Climate Change*, *2*(6), 462–467. https://doi.org/10.1038/nclimate1389

MacDonald, A., Scarrott, C. J., Lee, D., Darlow, B., Reale, M., & Russell, G. (2011). A flexible extreme value mixture model. *Computational Statistics and Data Analysis*, *55*(6), 2137–2157. https://doi.org/10.1016/j.csda.2011.01.005

Méndez, F. J., Menéndez, M., Luceño, A., & Losada, I. J. (2006). Estimation of the long-term variability of extreme significant wave height using a time-dependent Peak Over Threshold (POT) model. *Journal of Geophysical Research*, *111*, C07024. https://doi.org/10.1029/2005JC003344

Menéndez, M., Méndez, F. J., Losada, I. J., & Graham, N. E. (2008). Variability of extreme wave heights in the northeast Pacific Ocean based on buoy measurements. *Geophysical Research Letters*, *35*, L22607. https://doi.org/10.1029/2008GL035394

Menéndez, M., & Woodworth, P. L. (2010). Changes in extreme high water levels based on a quasi-global tide-gauge data set. *Journal of Geophysical Research*, *115*, C10011. https://doi.org/10.1029/2009JC005997

Merz, B., Kreibich, H., Schwarze, R., & Thieken, A. (2010). Review article "assessment of economic flood damage". *Natural Hazards and Earth System Sciences*, *10*(8), 1697–1724. https://doi.org/10.5194/nhess-10-1697-2010

Moftakhari, H. R., AghaKouchak, A., Sanders, B. F., Feldman, D. L., Sweet, W., Matthew, R. A., & Luke, A. (2015). Increased nuisance flooding due to sea-level rise: Past and future. *Geophysical Research Letters*, *42*, 9846–9852. https://doi.org/10.1002/2015GL066072

Moftakhari, H. R., AghaKouchak, A., Sanders, B. F., Allaire, M., & Matthew, R. A. (2018). What is nuisanceflooding? Defining and monitoring an emergingchallenge. *Water Resources Research*, *54*, 4218–4227. https://doi.org/10.1029/2018WR022828

Moftakhari, H. R., AghaKouchak, A., Sanders, B. F., & Matthew, R. A. (2017). Cumulative hazard: The case of nuisance flooding. *Earth's Future*, *5*(2), 214–223. https://doi.org/10.1002/2016EF000494

Moftakhari, H. R., Salvadori, G., AghaKouchak, A., Sanders, B. F., & Matthew, R. A. (2017). Compounding effects of sea level rise and fluvial flooding. *Proceedings of the National Academy of Sciences*, *114*(37), 9785–9790. https://doi.org/10.1073/pnas.1620325114

Mudersbach, C., & Jensen, J. (2010). Nonstationary extreme value analysis of annual maximum water levels for designing coastal structures on the German North Sea coastline. *Journal of Flood Risk Management*, *3*(1), 52–62. https://doi.org/10.1111/j.1753-318X.2009.01054.x

Nicholls, R., & Cazenave, A. (2010). Sea-level rise and its impact on coastal zones. *Science*, *328*(August). https://doi.org/10.1126/science.1185782

Niroomandi, A., Ma, G., Ye, X., Lou, S., & Xue, P. (2018). Extreme value analysis of wave climate in Chesapeake Bay. *Ocean Engineering*, *159*(November 2017), 22–36. https://doi.org/10.1016/j.oceaneng.2018.03.094

NOAA. (2014). National Weather Service Instruction 10–320. Surf Zone Forecast & Coastal/Lakeshore Hazard Services.

Noto, L. V., & La Loggia, G. (2009). Use of L-moments approach for regional flood frequency analysis in Sicily, Italy. *Water Resources Management*, *23*(11), 2207–2229. https://doi.org/10.1007/s11269-008-9378-x

Obeysekera, J., Park, J., Irizarry-Ortiz, M., Barnes, J., & Trimble, P. (2013). Probabilistic projection of mean sea level and coastal extremes. *Journal of Waterway, Port, Coastal, and Ocean Engineering*, *139*(2), 135–141. https://doi.org/10.1061/(ASCE)WW.1943-5460.0000154

Purvis, M. J., Bates, P. D., & Hayes, C. M. (2008). A probabilistic methodology to estimate future coastal flood risk due to sea level rise. *Coastal Engineering*, *55*(12), 1062–1073. https://doi.org/10.1016/j.coastaleng.2008.04.008

Rahmstorf, S. (2007). A semi-empirical approach to projecting future sea-level rise. *Science*, *315*(January), 368–370.

Rahmstorf, S., & Coumou, D. (2011). Increase of extreme events in a warming world. *Proceedings of the National Academy of Sciences*, *108*, 17,905–17,909. https://doi.org/10.1073/pnas.1101766108

Ray, R. D., & Foster, G. (2016). Future nuisance flooding at Boston caused by astronomical tides alone. *Earth's Future*, *4*(12), 578–587. https://doi.org/10.1002/2016EF000423

Roth, M., Buishand, T. A., Jongbloed, G., Klein Tank, A. M. G., & Van Zanten, J. H. (2012). A regional peaks-over-threshold model in a nonstationary climate. *Water Resources Research*, *48*, W11533. https://doi.org/10.1029/2012WR012214

Salas, J. D., & Obeysekera, J. (2014). Revisiting the concepts of return period and risk for nonstationary hydrologic extreme events. *Journal of Hydrologic Engineering*, *19*(3), 554–568. https://doi.org/10.1061/(ASCE)HE.1943-5584.0000820

Stephens, S. A., Bell, R. G., & Lawrence, J. (2018). Developing signals to trigger adaptation to sea-level rise. *Environmental Research Letters*, *13*, 104,004.

Sweet, W. V., Dusek, G., Obeysekera, J., & Marra, J. J. (2018). Patterns and projections of high tide flooding along the U.S. coastline using a common impact threshold. *NOAA Tech. Rep. NOS CO-OPS 44p.*, (February).

Sweet, W. V., Kopp, R. E., Weaver, C. P., Obeyskera, J., Horton, R. M., Thieler, E. R., & Zervas, C. (2017). Global and regional sea level rise scenarios for the United States, (January).

Sweet, W. V., & Park, J. (2014). From the extreme to the mean: Acceleration and tipping points of coastal inundation from sea level rise. *Earth's Future*, *2*(12), 579–600. https://doi.org/10.1002/2014EF000272

Sweet, W. V., Park, J., Marra, J., Zervas, C., & Gill, S. (2014). Sea level rise and nuisance flood frequency changes around the United States. *NOAA Technical Report NOS CO-OPS 073*, (June), 58. https://doi.org/10.13140/2.1.3900.2887

Tebaldi, C., Strauss, B. H., & Zervas, C. E. (2012). Modeling sea level rise impacts on storm surges along US coasts. *Environmental Research Letters*, *7*(1). https://doi.org/10.1088/1748-9326/7/1/014032

Vandenberg-Rodes, A., Moftakhari, H. R., AghaKouchak, A., Shahbaba, B., Sanders, B. F., & Matthew, R. A. (2016). Projecting nuisance flooding in a warming climate using generalized linear models and Gaussian processes. *Journal of Geophysical Research: Oceans*, *121*, 1–15. https://doi.org/10.1002/2016JC012084

Vousdoukas, M. I., Mentaschi, L., Feyen, L., & Voukouvalas, E. (2017). Extreme sea levels on the rise along Europe's coasts. *Earth's Future*, 1–20. https://doi.org/10.1002/2016EF000505

Wahl, T. (2017). Sea-level rise and storm surges, relationship status: Complicated! *Environmental Research Letters*, *12*(11), 111001.

Wahl, T., Jain, S., Bender, J., Meyers, S. D., & Luther, M. E. (2015). Increasing risk of compound flooding from storm surge and rainfall for major US cities. *Nature Climate Change*, *5*(12), 1093–1097. https://doi.org/10.1038/nclimate2736

Walsh, J., Wuebbles, D., Hayhoe, K., Kossin J., Kunkel K., Stephens G., et al. (2014). Our changing climate. Climate Change Impacts in the United States: The Third National Climate Assessment, J. M. Melillo, Terese (T.C.) Richmond, and G. W. Yohe, Eds., U.S. Global Change Research Program. https://doi.org/10.7930/J0KW5CXT

Wolf, J., & Woolf, D. K. (2006). Waves and climate change in the north-east Atlantic. *Geophysical Research Letters*, *33*, L06604. https://doi.org/10.1029/2005GL025113

Xu, S., & Huang, W. (2008). Frequency analysis for predicting 1% annual maximum water levels along Florida coast, US. *Hydrological Processes*, *22*, 4507–4518. https://doi.org/10.1002/hyp.7051